Effect of interpass temperature on properties of high-strength weld metals

by Mike Lord, Gill Jennings and Every, Great Britain

Abstract

High-strength weld metals frequently have a microstructure consisting of martensite or a mixture of martensite and acicular ferrite. The alloying of the weld metal has to be designed so that sufficient hardenability to generate the required microstructure during cooling is obtained. It has been observed that the yield strength of such alloys can exhibit considerable variation in the range of 700-950 MPa for the same consumable electrode. The work presented here reveals one reason for these variations — that the cooling curve of the weld is close to the limit of hardenability of the material. This means that the microstructure obtained becomes sensitive to variations in the interpass temperature in multirun welds.

Introduction

Making a high-strength steel using a variety of well-established strengthening mechanisms is a straightforward procedure. Achieving toughness, which is the ability of the metal to absorb energy during fracture, is far more difficult. The essence of most alloy design is to obtain a reasonable compromise between strength and toughness.

Unlike wrought steels, welds cannot usually be processed to enhance the microstructure and properties once the joint is completed. Many welds that are used for structural steels cannot even be heat treated after deposition. As a result, there are limitations to the maximum strength that can usefully be exploited. A high-strength weld is therefore currently limited to a yield stress of about 900 MPa for most practical circumstances.

Untempered microstructures capable of resisting deformation at such large stresses are based on martensite or on mixtures of martensite/bainite/acicular ferrite. The alloys must therefore contain a sufficient content of austenite-stabilising elements consistent with the hardenability required to avoid other phase transformations. At the same time, the carbon concentration must be minimised to avoid excessive hardness when the weld is deposited. So, elements such as manganese, nickel, chromium and molybdenum are added as they improve hardenability and yet do not excessively strengthen the steel. A typical weld metal composition for manual metal arc welding is therefore:
Fe-0.05C-0.5Si-1Mn-3Ni-0.5 Cr-0.5Mo wt%
with a strength of about 900 MPa and a Charpy notch toughness at –60°C of about 60 J.

It has been found that the mechanical properties of this and similar higher strength welds are variable, even though the chemical composition of the deposit does not change (1). In particular, the yield strength can vary (150 MPa), whereas the ultimate tensile strength does not vary as much. This is unsatisfactory from the customer's point of view and indeed for the electrode manufacturer who has to supply electrodes to specification.

The purpose of the present work was to investigate the variability in the mechanical properties of these high-strength weld deposits.

Experimental details

Weld specifications

An experimental weld (multirun MMA) was fabricated according to ISO 2560 using a 20 mm thick plate filled with 30 runs (three beads per layer). An interpass temperature of 250°C was used.

C	Mn	Si	Cr	Mo	Ni
05	2.0	0.3	0.4	0.6	3.0

Table 1 Concentration (in weight%) of the major alloying elements in the experimental weld.

This configuration causes little dilution of the weld metal, thereby permitting the accurate isolation and measurement of weld metal properties. Welding was performed at 24 V, 180 A and a heat input of 1kJ/mm. The nominal composition data for the weld are shown in Table 1.

Mechanical testing

Two tensile specimens and 20 Charpy-V impact specimens were machined. Prior to tensile testing, the specimens were degassed at 250°C for 16 hours. The impact specimens were tested at four different temperatures and five specimens were tested at each temperature. The test temperatures were +20°C, 0°C, –20°C, –40°C and –60°C.

Specimens for microscopy

Specimens for light microscopy were produced by hot mounting the weld material in bakelite. Following grinding and polishing down to a 1 μm diamond grit finish, the samples were etched with 2% nital.

Transmission electron microscopy samples were made from cylindrical rods with a diameter of 3 mm machined from sections of weld metal. The final preparations were performed using a twin jet electropolisher at ambient temperature and a potential of 50V. The electropolishing solution comprised 5% perchloric acid, 10% glycerol and 85% ethanol (Brammar, 1965). Imaging was performed in a Philips 400ST transmission electron microscope operating at 120 kV.

$R_{p0.2}$ (MPa)	R_m (MPa)	A_5 (%)	Z (%)	Impact toughness (J)				
				+20°C	0°C	−20°C	−40°C	−60°C
872	922	22	67	102	95	87	79	64

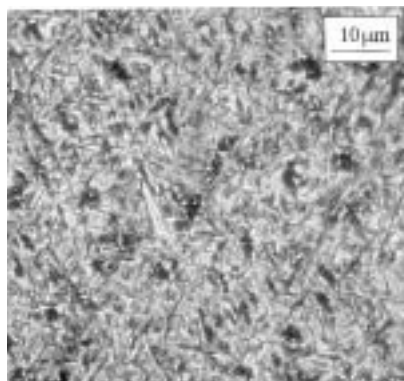Table 2. Results of mechanical testing.

Figure 1. Dark-field optical micrograph showing little resolvable detail.

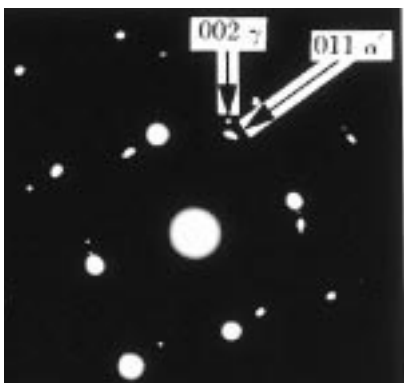Figure 2. TEM micrograph showing the bainitic microstructure of the weld metal.

Figure 3. Electron diffraction pattern showing ferrite and austenite spots in an approximate Kurdjumov-Sachs orientation.

Dilatometry

A Thermecmastor Z thermo-mechanical simulator was used to study the phase transformations occurring within the weld metal as a function of the applied cooling rates. The transformations were monitored using laser dilatometry. Specimens for use in the simulator were machined into cylinders with a length of 12 mm and a diameter of 8 mm. A hole with a diameter of 5 mm was drilled along the central length of the specimens, the reduction in material volume producing more accurate data. Heating the specimens was effected via an induction coil and cooling was similarly controlled using a combination of induction coil heating and jets of helium quenching gas.

In the production of a continuous cooling transformation (CCT) curve, the specimens were austenitised at 1,200°C for 10 minutes in order to reduce the effect of the austenite microstructure before each specific cooling cycle was applied.

Results

Mechanical testing

The results of the tensile and impact toughness tests are presented in Table 2.

Microstructure

Light microscopy has a resolution of about 0.5 µm at most. Observations revealed apparently plate-like features, but they were believed to represent clusters of plates which are much finer. The fine structure could not really be revealed and was not found to change much with its position within the multirun weld (Figure 1).

Thin foil observations using transmission electron microscopy revealed a fine microstructure comprising bainite plates with a width of the order of 0.3 µm. A typical TEM micrograph is shown in Figure 2. Electron diffraction proved the presence of retained austenite films between the bainitic ferrite plates. The crystallographic orientation between the austenite and adjacent ferrite was found to be consistent with that expected from a rational Kurdjumov-Sachs (KS) relationship (Figure 3).

The alloy contains a fairly low carbon concentration, so the ready observation of reasonably thick retained austenite films might be considered surprising at first sight. However, carbon is partitioned from the bainite after it stops growing and this stabilises the austenite which is enriched in carbon (2). In fact, the observation of these thick films can be safely taken to indicate the presence of bainite, which in low-alloy steels can be difficult to distinguish from martensite. Carbide precipitation was never found in spite of extensive investigations.

Dilatometry to produce a CCT curve

Further experiments using dilatometry were conducted to verify that the fine plates with intervening austenite represented bainite rather than martensite. If the observed transformation temperature remains constant for different cooling rates, it can be concluded that the final microstructure must be martensitic, since the martensite-start (Ms) temperature does not depend on the cooling rate for low-alloy steels (3). On the other hand, the temperature at which a detectable fraction of bainite forms does depend on the cooling rate, because the overall kinetics of the reaction can be described in terms of a C curve on a continuous cooling transformation (CCT) diagram.

A CCT curve was produced by cooling specimens at various rates ranging from 100°C/s to 0.05°C/s. Figure 4 shows the experimental CCT curve, along with the calculated Ms temperature (4) and a calculated MMA weld bead cooling rate with an interpass temperature of 250°C (5) denoted '250°C ITP'.
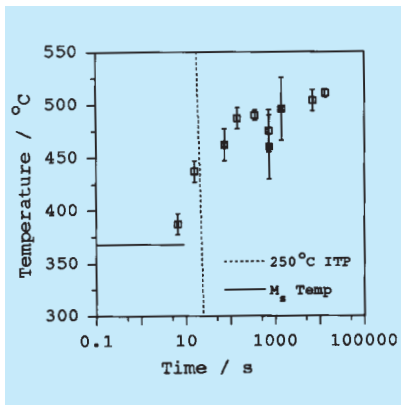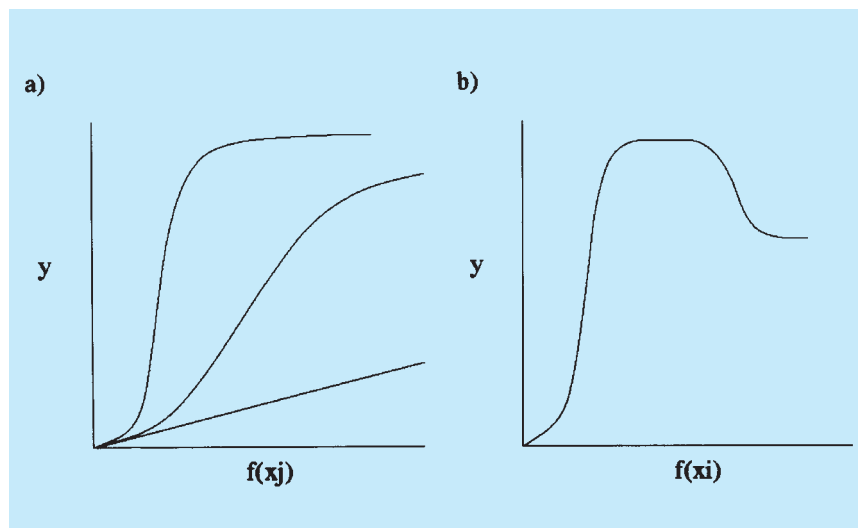
Figure 4 Experimental CCT curve.

Figure 5 a) Three different hyperbolic tangent functions; the "strength" of each depends on the weights. (b) A combination of two hyperbolic tangents to produce a more complex model. Details about the methodology can be found in David Mackay's article in Mathematical Modelling of Weld Phenomena III.

The calculated weld bead cooling rate clearly cuts the CCT curve beyond the limit of hardenability in a region which should produce a bainitic microstructure. TEM micrographs showed fine plates which confirm a displacive mechanism of transformation. These two curves intersect at a position at which the gradient of the CCT curve is very large. Consequently, small variations in the cooling rate of the material could drastically alter the transformation temperature and thereby the resultant mechanical properties. This hypothesis led to questions concerning the possible causes of such variations. The problem was approached using a sophisticated method of pattern recognition, known more generally as neural network analysis.

Neural network: the method

There are difficult problems (such as welding) in which the general concepts might be understood but which are not as yet amenable to rigorous mathematical treatment. Most people are familiar with regression analysis where data are best-fitted to a specified relationship which is usually linear. The result is an equation in which each of the inputs xj is multiplied by a weight wj. The sum of all such products and a constant C then gives an estimate of the output y =

$$w_1 \cdot x_1 + w_2 \cdot x_2 + \ldots + C$$

It is well understood that there are dangers in using such relationships beyond the range of fitted data.

A more general method of regression is neural network analysis (6–9). As before, the input data xj are multiplied by weights, but the sum of all these products forms the argument of a hyperbolic tangent. The output y is therefore a non-linear function of xj; the function which is usually chosen is the hyperbolic tangent because of its flexibility. The exact shape of the hyperbolic tangent can be varied by altering the weights (Figure 5a). Further degrees of non-linearity can be introduced by combining several of these hyperbolic tangents (Figure 5b), so that the neural network method is able to capture almost arbitrarily non-linear relationships. For example, it is well known that the effect of chromium on the microstructure of steels is quite different at large concentrations than in dilute alloys. Standard regression analysis cannot cope with such changes in the form of relationships.

One potential difficulty when it comes to the use of powerful regression methods is the possibility of overfitting data (Figure 6). For example, it is possible to produce a neural network model for a completely random set of data. To avoid this difficulty, the experimental data can be divided into two sets, a training dataset
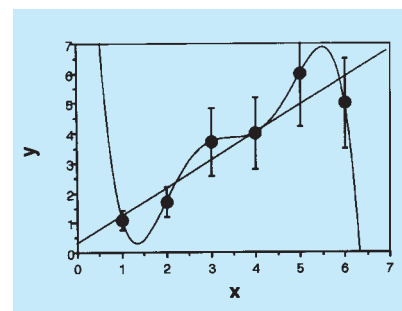

Figure 6 A complicated model may overfit the data. In this case, a linear relationship is all that is justified by the noise in the data.

and a test dataset. The model is produced using only the training data. The test data are then used to check that the model behaves when presented with previously unseen data.

Neural network models in many ways mimic human experience and are capable of learning or being trained to recognise the correct science rather than nonsensical trends. Unlike human experience, these models can be transferred readily between generations and steadily developed to make design tools of lasting value. These models also impose a discipline on the digital storage of valuable experimental data, which may otherwise be lost with the passage of time.
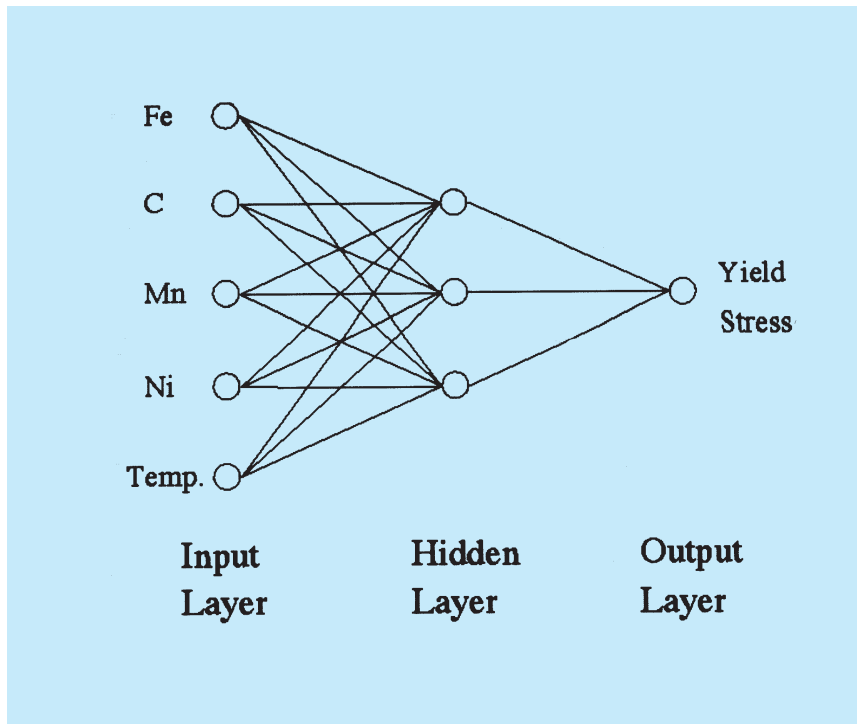
Figure 7 Graphical representation of a neural network. Some examples of input node parameters are also presented.

Neural network structure

While there are many varieties of neural network, the type used in this work can be expressed diagramatically as shown below. In this case, the network is composed of three "layers". The first layer contains the model input data provided by the user, such as compositional details (simply as normalised values), the second "hidden" layer is an internal stage and describes the degree of complexity of the substructure of the network. The third "output" layer contains the predicted value of the parameter in question when running a calculation. Figure 7 shows a simplified network with five example input parameters.

The circles within the diagram are called nodes or units, so here there are five "input nodes". The hidden layer comprises three hidden nodes and the output layer is simply a single output node. The number of nodes in the hidden layer limits the complexity of the possible relationships between the input and output nodes. The lines connecting the nodes represent mathematical functions performed on the values as they pass from the input to the output layer. In this network, hyperbolic tangent functions are utilised, as they are always single valued, exhibit both near-linear and non-linear regions and are relatively easy to manipulate. When performing a "prediction" using a neural network, data are operated on by a hyperbolic tangent function as they are passed between the input and hidden layers. This function is of the form:-

$$h_i = \tanh \left(\sum w_{ij}^{(1)} x_j + \theta_i^{(1)} \right)$$

where xj are the normalised values of the input variables, $w_{ij}^{(1)}$ are a set of "weights" associated with each input and hidden unit and $\theta_i^{(1)}$ are bias values analogous to constants found in linear regression.

The values hi are transferred from the hidden layer to the output layer via a second function of the form:–

$$y = \sum_i w_i^{(2)} h_j + \theta^{(2)}$$

where y is the value of the output node (e.g. yield strength), $w_i^{(2)}$ are a second set of weights and $\theta^{(2)}$ is a further constant known as a 'bias'.

The numerous weighting coefficients and constants ($w_{ij}^{(1)}$, $\theta_i^{(1)}$, $w_i^{(2)}$ and $\theta^{(2)}$) are required in order to provide the flexibility to calculate accurate output values from input data. At the heart of the neural network technique there are algorithms designed to evaluate these coefficients and constants in order to produce satisfactory results.

Training the network

Training involves repeatedly exposing the training algorithms to data for the network inputs (e.g. compositions) and, crucially, the output (e.g. yield stress). The data must come from a database relevant to the particular application in question. The quality of this database determines, at least in part, the final accuracy of the network predictions. The required size of the database may vary depending on the complexity of the problem that is being modelled. In general, the larger the amount of accurate data, the better the predictions of the resulting network. The training algorithms refine the coefficients and variables in the above equations by comparing the predicted and actual output values of the output node. Through a complicated back-propagation process, the computer program attempts to reduce the differences between predicted and actual values until they reach acceptably low levels. There is an additional problem with "overtraining", which means that the network can learn the examples in the dataset too well and will then be unable to predict values for different unseen compositions. This is analogous with fitting a complicated curve to a set of points that lie on a straight line, where the experimental errors have been modelled into the network rather than just the trend. Using a number of different hidden nodes and training on a randomly-selected half of the available data, the best network can be picked to strike a balance between modelling real trends and overtraining on noise in the data. The second half of the dataset is used to compare the predictions of this trained network (Figure 8). Ideally, plots of predicted versus measured values for both the training and testing halves of the dataset should contain equal degrees of scatter.
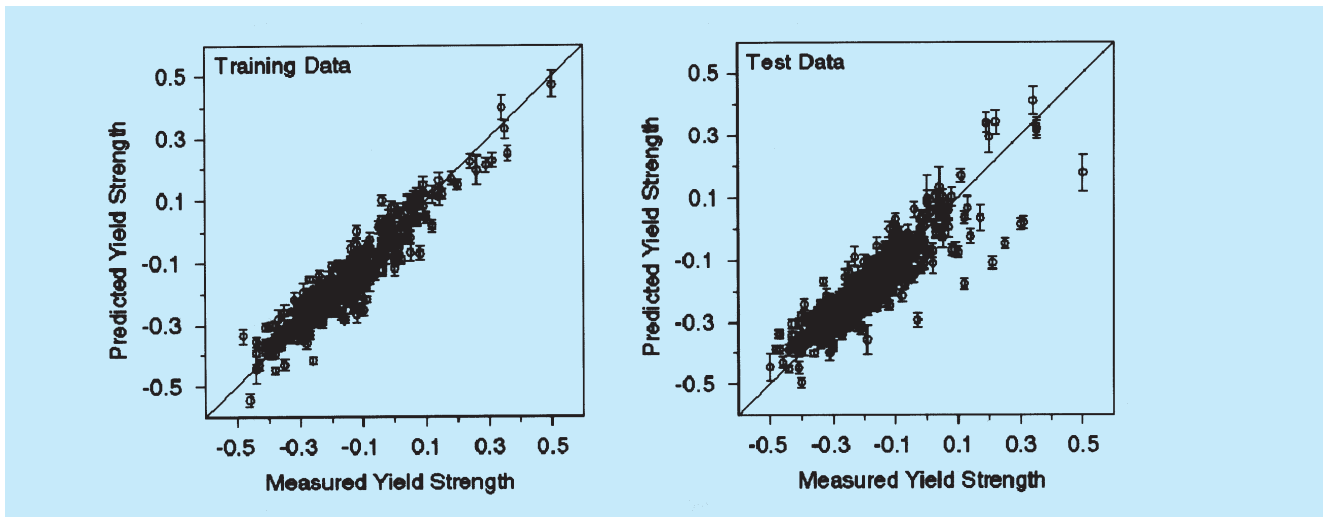
Figure 8 The similar appearance of both training and testing data graphs indicates a good balance between predicting trends and modelling noise.

Two types of network were trained on data from 770 welds drawn from a variety of sources, the first giving yield stress as an output, the second ultimate tensile strength (10). Nineteen input variables were provided for each of these welds, fifteen of which were due to alloying elements, while the remaining four were due to the heat input, interpass temperature and tempering time and temperature values if applicable.

A number of different networks were trained and tested. In the case of the yield stress models, the five best models were then combined to create a "committee". A committee of networks is superior to a single one as, collectively, they should capture the trends in the data more effectively. Each network within the committee was retrained on the complete dataset to provide greater accuracy before committee predictions were made. Similarly, a committee of four models was used in the predictions of ultimate tensile strength.

Investigation of tensile strength effects
As stated earlier, previous analyses of the weld microstructure had provided little insight into the cause of the observed variations in strength. However, dilatometer data in the form of a CCT curve had shown that typical MMA measured cooling rates could fall in a critical region. The hardenability of the weld metal caused plotted weld cooling rates
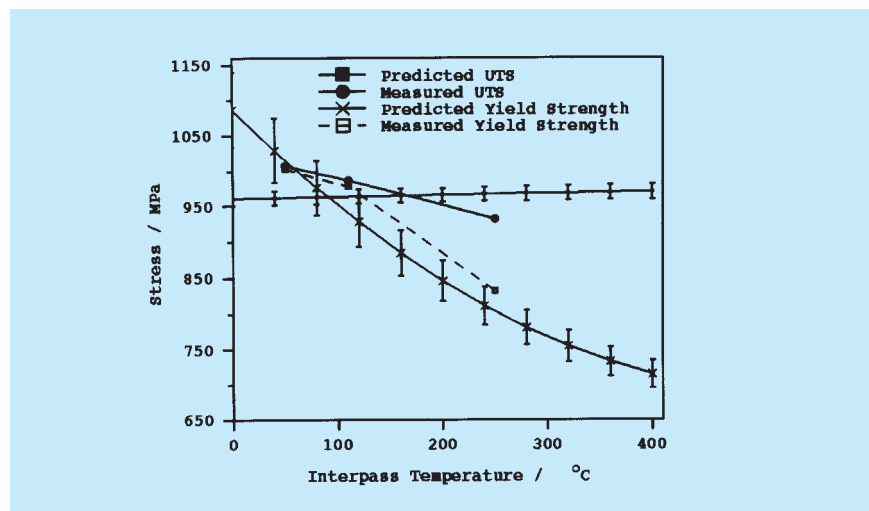

Figure 9 Predicted and measured yield and ultimate tensile strengths as a function of interpass temperature.

to fall close to the "nose" of the bainite curve in a region of particularly high gradient. A calculation of this kind indicated that small variations in the weld cooling rate could considerably affect the transformation temperature. It was thought likely that such a variation in the displacive transformation temperatures of the material would have a large enough effect significantly to alter mechanical properties. The majority of the transformation occurring at a higher temperature, for example, would lead to a reduction in yield stress, as the effects of diffusion on both carbon mobility and dislocations are temperature dependent.

Compositional variations alone could not be held responsible for the large variations in yield strength reported for this materi-

al. It would seem more plausible to consider process parameters as being responsible. This rationale eventually led to the identification of the interpass temperature as a possible candidate for causing the strength variations. Large joints comprise many passes in order to deposit the required amount of material. Welds under construction cool at a rate determined by their environment, such as the degree to which the surrounding material acts as a heat sink and the temperature of those surroundings. If the interpass temperature is high, a subsequently deposited bead will cool at a reduced rate which, it was surmised, may be significantly lower, depending upon the temperature. The trained neural network as a research tool was now useful as it provided a means of

testing this theory without having to perform lengthy experiments with real welds.

Predictions were made after choosing a range of interpass temperatures. The results were so significant that it was decided to perform physical experiments in order to test the predictions. A series of three welds, using the high-strength steel electrode, were produced with carefully monitored interpass temperatures of 50°C, 110°C and 250°C. The results of the predictions and the tensile tests on the new welds are presented in Figure 9.

There is a clearly predicted divergence in the yield stress and UTS of the weld metal as a function of the interpass temperature, a divergence of approximately 1 MPa per °C. A second feature of the predicted curves is the crossing over of yield stress and UTS predictions below about 90°C. This is an example of situations in which caution should be exercised when using neural network predictions. The network clearly has no knowledge of the laws that determine the behaviour of the system it is modelling and consequently the user must always ensure that they make physical sense.

In this case, it is to be expected that the gap between yield stress and UTS reduces to a few MPa at interpass temperatures approaching ambient temperatures. The experimental results clearly show a divergence in yield stress and UTS similar to that predicted. In this case, the yield stress model appears to be more accurate, as the UTS values appear to reduce as a function of interpass temperature, whereas the UTS network predicts a slight increase as a function of interpass temperature. It is the yield stress values that are of most interest, particularly as they approach the UTS values at low interpass temperatures and fall off rapidly as this temperature is increased. Conventionally, it is desirable to have the yield stress to UTS ratio closer to 0.8 in the interests of producing ductile failure in the event of the joint being overloaded. This ratio is only realised at interpass temperatures of above 200°C. These

results provide a probable cause for the varying properties in weld metals of these kinds. Historically, the interpass temperature has often not been rigidly monitored and it is clearly imperative with this weld composition that precautions are taken.

The results of these experiments have enabled a recommendation to be made detailing the strict adherence to the specified interpass temperature.

Conclusions

There are three major conclusions that can be drawn from this work. By comparing transmission electron microscopy and diffraction data with measurements of transformation temperatures using dilatometry, it has been possible to prove that the high-strength weld cannot be fully martensitic at the cooling rates typical of welding. The microstructure will instead consist of a mixture of martensite and bainite, the latter consisting of bainitic ferrite separated by carbon-enriched films of retained austenite. These methods are recommended in circumstances where it is otherwise difficult to distinguish bainite and martensite (i.e. when the microstructure is very fine and the carbon concentration so small that carbide precipitation is prevented).

The second conclusion is that difficulties are to be expected with respect to the mechanical properties when the bainite and martensite transformations occur at temperatures which are not much above the nominal interpass temperature. This is because the cooling rate of the weld between the bainite and martensite start temperatures becomes very sensitive to the interpass temperature. Failure accurately to control the interpass temperature leads to large variations in the microstructure and hence in the mechanical properties.

Finally, a neural network model has been shown to be reliable in predicting the effect of the interpass temperature on strength, both in terms of the absolute values and in the relative variation in the yield and ultimate

tensile strengths. It is particularly encouraging that the model predicted that the difference between these two measurements of strength is a function of the interpass temperature.

References
1 P. T. Oldland, C. W. Ramsay, D. K. Matlock, D. L. Olson, Welding Research Supplement, April 1989, pp 158-167

2 H. K. D. H. Bhadeshia, Bainite in Steels, Institute of Materials, 1992, 154-157

3 R. Kumar, Physical Metallurgy of Iron and Steel, Asia Publishing House,1968, 200-256

4 H. K. D. H. Bhadeshia, Metal Science, 15, 1981, 175-180

5 L.-E. Svensson, B. Gretoft, H. K. D. H. Bhadeshia, Scand. J. Metallurgy,15, 1986, 97-103

6 D. J. C. MacKay, Neural Computation, 4, 3, 1992a, 415-447

7 D. J. C. MacKay, Neural Computation, 4, 3, 1992b, 448-472

8 D. J. C. MacKay, Neural Computation 4, 5, 1992c, 698-714

9 D. J. C. MacKay, Darwin College Journal, Cambridge, 1993, 81

10 T. Cool, H. K. D. H. Bhadeshia, D. J. C. MacKay, Mat. Sci. Eng. A, 223, 1997, 186-200

About the author

Mike Lord graduated from Cambridge University with a degree in Natural Science, specialising in Materials Science 1995. He then joined the Phase transformation research group in Cambridge to do a PhD. His subject was phase transformations and properties of high strength weld metals. His work was sponsored by Esab and EPSRC. Mr Lord was awarded the Granjon prize 1998, Category 2 by IIW for his paper "Interpass temperature and the welding of strong steels". Mr Lord is presently working at Gill Jennings and Every, training to become a British and European Patent Attorney.